PAPER

Numerical model of halite precipitation in porous sedimentary rocks adjacent to salt diapirs

To cite this article: Shiyuan Li *et al* 2017 *J. Geophys. Eng.* **14** 1160

IOP Publishing Journal of Geophysics and Engineering
J. Geophys. Eng. **14** (2017) 1160–1166 (7pp) https://doi.org/10.1088/1742-2140/aa73f9

Numerical model of halite precipitation in porous sedimentary rocks adjacent to salt diapirs

Shiyuan Li[1,2,6], **Lars Reuning**[3], **Gabriele Marquart**[4], **Yan Wang**[1] and **Pengyun Zhao**[5]

[1] College of Petroleum Engineering, China University of Petroleum, Beijing, People's Republic of China
[2] State Key Laboratory of Oil and Gas Resources and Exploration, Beijing, People's Republic of China
[3] Geological Institute, RWTH-Aachen, Germany
[4] Applied Geophysics and Geothermal Energy Institute, RWTH-Aachen, Germany
[5] Eleventh Oil Production Plant, Changqing Oilfield, 751500, Xi'an, People's Republic of China

E-mail: lishiyuan1983@cup.edu.cn

Received 18 April 2016, revised 29 March 2017
Accepted for publication 18 May 2017
Published 18 August 2017

Abstract

Salt diapirs are commonly seen in the North Sea. Below the Zechstein Group exist possibly overpressured salt-anhydrite formations. One explanation as to the salt precipitation in areas with salt diapirs is that salt cementation is thermally driven and occurs strongly in places adjacent to salt diapirs. This paper assumes that the sealing effect of the cap rock above the salt formations is compromised and overpressured fluids, carrying dissolved minerals such as anhydrite ($CaSO_4$) and salt mineral components (NaCl of halite), flow into the porous sedimentary layers above the salt formations. Additionally, a salt-diapir-like structure is assumed to be at one side of the model. The numerical flow and heat transport simulator SHEMAT-Suite was developed and applied to calculating the concentrations of species, and dissolution and precipitation amounts. Results show that the overpressured salt-anhydrite formations have higher pressure heads and the species elements sodium and chlorite are transported into porous sediment rocks through water influx (saturated brine). Halite can precipitate as brine with sodium and chlorite ions flows to the cooler environment. Salt cementation of reservoir rocks leads to decreasing porosity and permeability near salt domes, and cementation of reservoir formations decreases with growing distance to the salt diapir. The proposed approach in this paper can also be used to evaluate precipitation relevant to scaling problems in geothermal engineering.

Keywords: salt-anhydrite layer, halite precipitation, SHEMAT, porous sedimentary rock

(Some figures may appear in colour only in the online journal)

Introduction

Salt diapirs are commonly seen in the North Sea area (Van Gent *et al* 2011, Strozyk *et al* 2012). Below the Upper Permian Zechstein Group exist possibly overpressured salt and anhydrite formations (Reuning *et al* 2009, Kukla *et al* 2011). Salt formations and unconsolidated salt sediments can serve as hydrocarbon reservoirs, and salt diapirs are closely related to petroleum systems. However, halite cementation in the pore space can often result in low porosity and permeability in sedimentary formations (Dronkert and Remmelts 1996, Purvis and Okkerman 1996), and these processes are usually bonded to the nearby salt dome. Hence, studies on such topics are of considerable value. On the one hand, from the perspective of scientific research, it is important to predict salt cementation and explain the cementation mechanism in reservoirs around salt diapirs, in not only a qualitative but also a quantitative way. On the other hand, in terms of engineering significance, it is useful to evaluate the effects of salt cementation on formation properties before drilling.

One explanation as to the aforementioned phenomenon is that salt cementation occurs strongly in places adjacent to salt

[6] Author to whom any correspondence should be addressed.

diapirs due to temperature gradients. In order to capture the mechanism in not only a qualitative but also quantitative way, numerical models were established using SHEMAT (Clauser 2003), a fluid flow–heat transport and chemical calculation code similar to TOUGH (Battistelli *et al* 1997). This numerical simulator deals with the coupling problem of underground water flow, heat transfer and species transport, and is capable of providing good results for not only underground engineering but also geothermal engineering research (Prakash 2013, Swain *et al* 2015). Concerning reactive flows in hot aquifers, chemical reactions between reservoir rocks and fluids are important, because dissolution and precipitation of minerals can influence the properties of the reservoir, such as rock porosity and permeability (Kühn *et al* 1997, 1998, 2002). The chemical module (Kühn and Pape 2003) in SHEMAT can accurately calculate the concentration of each species as well as dissolution and precipitation amounts. In this paper, the chemical module was reprogrammed and embedded into the SHEMAT-Suite, which was the new version of SHEMAT developed five years ago. Compared with the previous version, the SHEMAT-Suite has extra functions and improved calculation stability. Fluid flow and chemical reaction can be combined on the basis of the fractal correlation between porosity and permeability (Pape *et al* 1999, 2000, Bartels *et al* 2002). Here we assume that sealing of the cap rock covering the salt diapir is compromised for some reason, and overpressured fluids, carrying dissolved minerals such as anhydrite ($CaSO_4$) and salt mineral components (NaCl of halite), are released into the porous sedimentary layers above the salt formations. Additionally, it is assumed that a salt-diapir-like structure is located at one side of the model. In our research the numerical flow and heat transport simulator SHEMAT (Clauser 2003) is applied to calculate the concentration of species and the amount of dissolution and precipitation.

The species concentration, and dissolution and precipitation amounts were calculated using the chemical module in the fluid flow and heat transfer simulator SHEMAT (Clauser and Villinger 1990, Clauser *et al* 1997, Clauser 2003), which is capable of characterizing the water–rock chemical interaction in fluid-saturated porous media. At each calculation time step, pressure, temperature and concentration are calculated through SHEMAT and are then transferred into the chemical module for further calculation regarding the chemical reaction. After the chemical reaction calculation, the updated pressure, temperature and concentration of reactive species or minerals are transferred again back to SHEMAT (Kühn and Pape 2003). As mentioned above, the reservoir properties, e.g. porosity and permeability, are affected by the chemical reactions between rocks and fluids. Hence, the mutual effects of fluid flow and chemical reactions can be described with the help of the correlation between the porosity and the mineral concentration (Pape *et al* 1999, 2000, Bartels *et al* 2002). The correlation can be expressed as follows:

$$\varnothing = \varnothing_0 + \varnothing_0(C_0 - C)\mathrm{V}_{\mathrm{mol}} \tag{1}$$

where C_0 is the initial mineral concentration; C represents the mineral concentration after chemical reactions; $\varnothing_0$ is the initial porosity; and $\mathrm{V}_{\mathrm{mol}}$ stands for the molar volume.

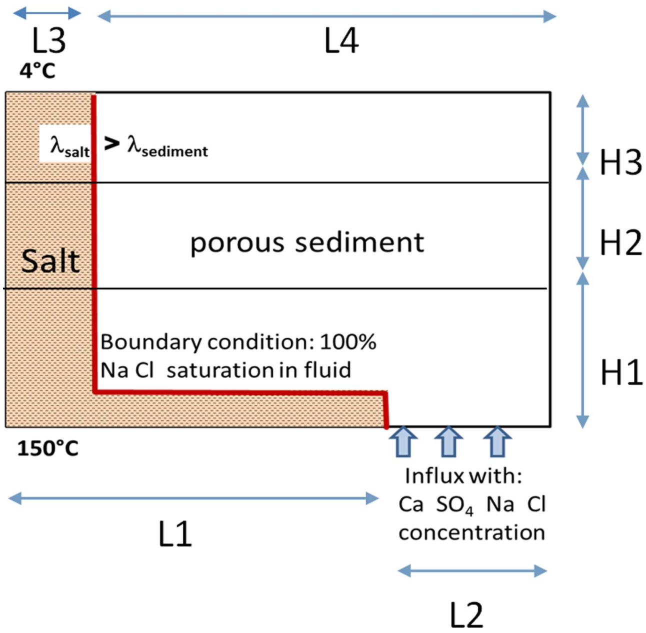

Figure 1. Model configurations of salts and multiple sedimentary formations.

Table 1. Geometrical parameters.

	L1	L2	H
Model	6500 m	3500 m	5000 m
	L3	L4	
Model	1500 m	8500 m	

The salt precipitation mechanism

The mechanisms of salt dome-induced plugging, which occurs much later in geological history than diagenesis, have been identified. The process is mainly controlled by temperatures (Van Bergen and Deleeuw 2001). The effects of pressures on salt precipitation are relatively small compared to the thermal ones, and are therefore neglected in this study.

The temperature-controlled mechanism is based on the fact that the salt solubility grows with the increase in temperatures. In other words, salts will precipitate when the saturated solution, or brine, is transported to an environment with lower temperatures. Therefore, this precipitation mechanism also depends strongly on the transport of brine. A more detailed description of the temperature-dominated salt distribution evolution is given below. The mineral concentration in fluids is a function of pressures and temperatures. The thermal conductivity of salts is much higher than that of sediments. Therefore temperatures of areas close to the salt diapir are different from those in other parts of the reservoir. Varied temperatures lead to diverse salt solubility. To sum up, salt precipitation occurs as the saturated solution flows into the cold zone around the salt diapir. Thus, variations in salt concentrations and precipitation in the pore space with different distances to the salt diaper are expected.

Table 2. Temperatures, pressures and concentrations.

	Head on top side	Head on bottom side	Head on influx
Model	5000 m	5000 m	5020 m
	Concentrations of sodium and chlorite at the top side	Concentrations of sodium and chlorite in in the salt dome	Concentrations of sodium and chlorite in the influx
Model	0.6 mol l^{-1}	7.0 mol l^{-1}	5.9 mol l^{-1}
	Heat flow through the bottom side	Temperature of the influx	
Model	$q = 0.065$ W m^{-2}	$T = 150$ °C	

Table 3. Porosity and permeability in the sedimentsand salt dome.

	Porosity in layer H1	Porosity in layer H2	Porosity in layer H3
Model	0.1	0.01	0.1
	Permeability of Layer H1	Permeability of Layer H2	Permeability of Layer H3
Model	10^{-15}	10^{-16}	10^{-15}
	Porosity of salts	Permeability of salts	
Model	0.001	10^{-18}	

Table 4. Thermal conductivity.

	Thermal conductivity of layer H1	Thermal conductivity of layer H2	Thermal conductivity of layer H3
Model	2.5	2.5	2.5
	Thermal conductivity of salts		
Model	5.5		

Table 5. Time scale and steps.

	Time scale and steps	Time scale and steps	Time scale and steps
Model	3.3 My 300 steps	6.6 My 600 steps	9.9 My 900 steps

Model configurations

It is assumed in this paper that sealing of the cap rock above the salt formations fails, and overpressured fluids with dissolved anhydrite mineral components ($CaSO_4$) and salt mineral components (NaCl) of halite migrate into the shallower porous sedimentary layers. Moreover, a salt-diapir-like structure is defined and positioned at one side of the model. The model has three formations with different porosity. The model geometry with a study area of 10 km × 5 km (figure 1) in the SHEMAT-Suite is based on Van Bergen and Deleeuw (2001). The pressure of the formations is assumed to be hydrostatic, and the temperatures are respectively 150 °C (bottom) and 4 °C (top). The salt-diapir-like structure is located at the left side of the model. The whole area is discretized with grids of size 5.0 m × 5.0 m. The entire simulation time is 3×10^{14} s (10 million years) in the case of halite precipitation, and three time scales are set for the case study of anhydrite. The properties of fluid flow, thermal rock, transport and reactions are separately provided. The influx is set as the saturated brine with 7000 mmol l^{-1} sodium and 7000 mmol l^{-1} chlorite.

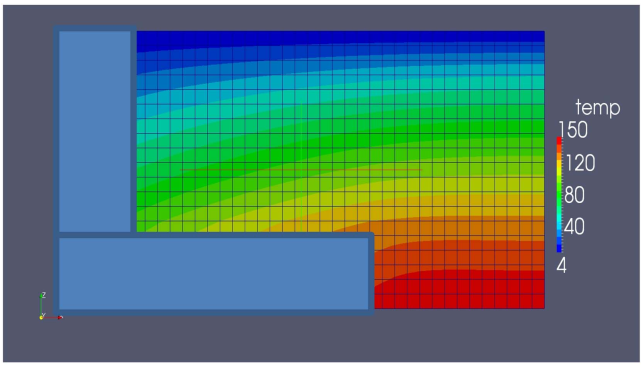

Figure 2. Temperature distribution in the porous sediment.

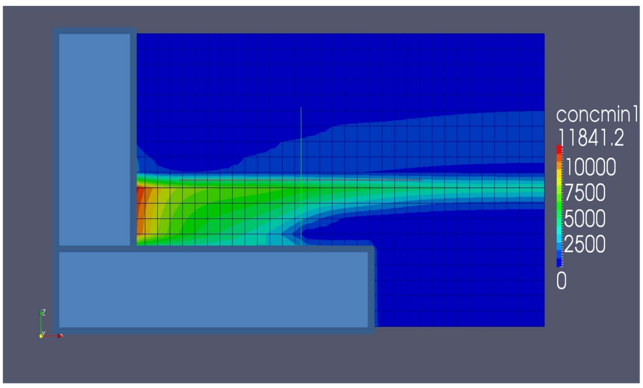

Figure 3. Salt precipitation and concentration distribution in the porous sediment.

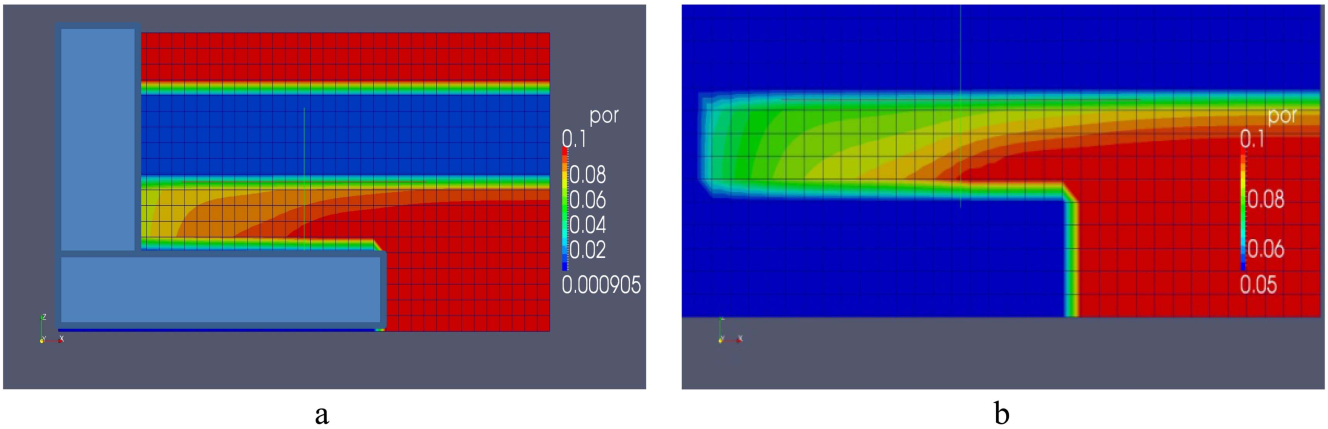

Figure 4. (a) Porosity distribution in the porous sediment. (b) Porosity distribution in the porous sediment; layer H1, increasing along the horizontal direction.

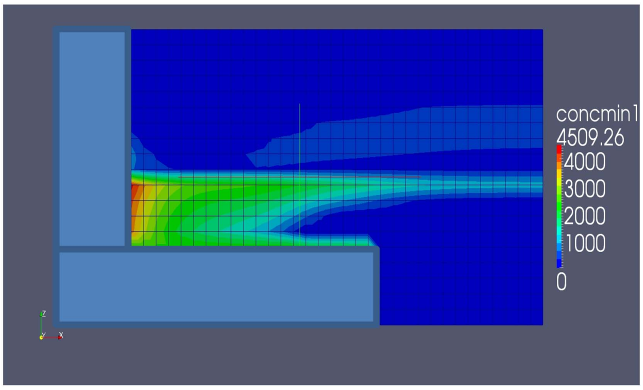

Figure 5. Temperature distribution in the porous sediment.

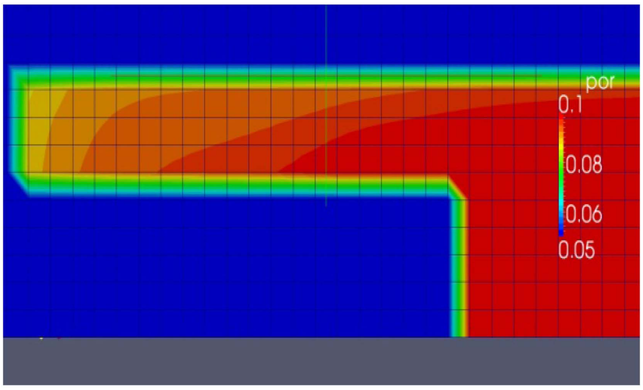

Figure 7. Porosity distribution in the porous sediment; layer H1.

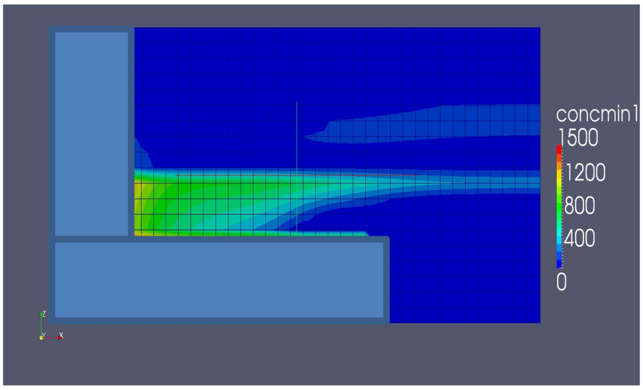

Figure 6. Salt precipitation and concentration distribution in the porous sediment.

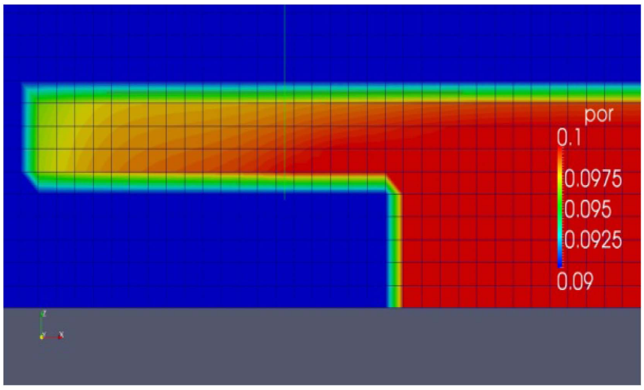

Figure 8. Porosity distribution in the porous sediment; layer H1, increasing along the horizontal direction.

As shown in figure 1, the left part is the salt diapir and the right part is the porous sedimentary formation. The right part includes multiple layers, which respectively have various porosity and permeability.

In terms of the model configuration, the following assumptions are made: (a) the porous sediments are filled initially with sea water; (b) the concentration of influx fluids of halite is slightly less than that of saturated fluids; and (c) the porosity of the sediments is 10% and permeability is 10^{-15}. The initial parameters are listed in the tables 1–5.

Results

The temperature gradient is clearly shown in figure 2, and it is also found that the temperatures of areas adjacent to the salt

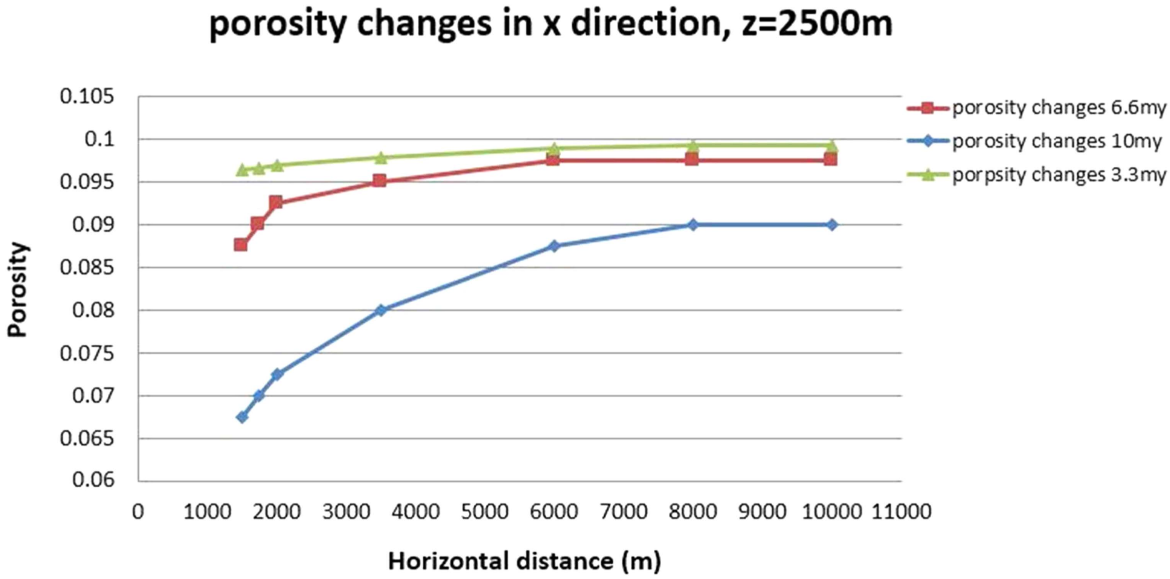

Figure 9. Porosity versus horizontal distance to the salt diapir (the reference position is the left edge of the model).

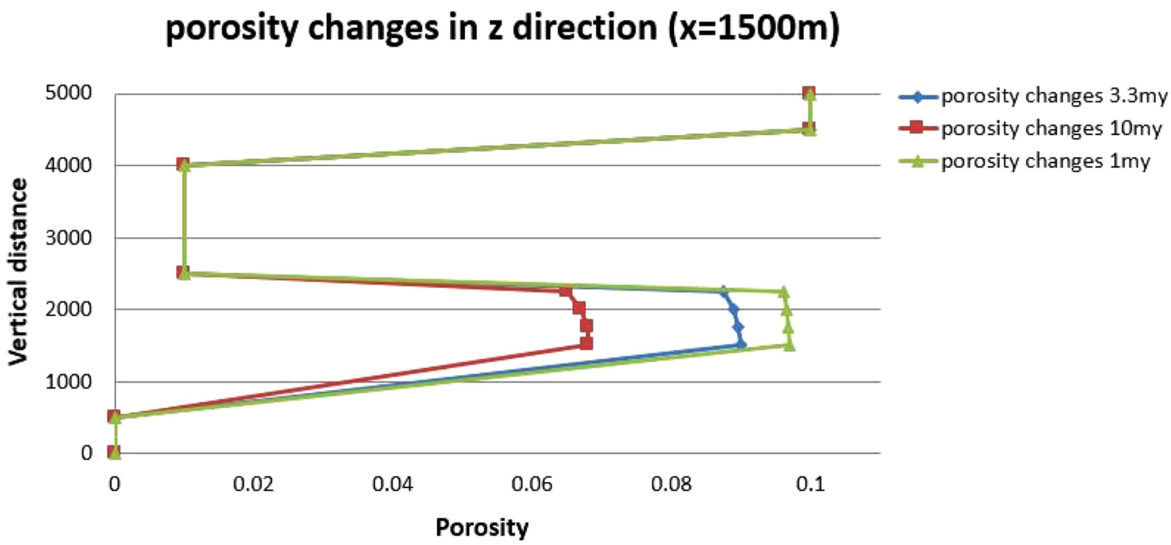

Figure 10. Porosity along the salt diapir versus vertical distance. Porosity increases from right to left in layer H1.

diaper are lower, due to the higher thermal conductivity of salts. The temperatures close to the salt diapir are about 40 °C lower than the temperatures along the right side of the model. After the salt-anhydrite-bearing water influx flows into the porous sediment, corresponding chemical reactions occur in 10 My, as the temperature gradient evolves. The concentration of precipitated salts reaches 11 841.2 mmol l^{-1} (figure 3), and the porosity accordingly decreases due to the fact that the pore space is occupied by newly emerging precipitated solids. It is illustrated in figure 4(a) that the gradient orientation of porosity is horizontal, with porosity next to the salt diaper around 0.07 and that of the right end of the model around 0.09 (figure 4(b)).

In terms of the first two cases, respectively having a time scale of 3.3 My and 6.6 My, the temperatures of areas adjacent to the salt diapir are still lower, which can also be attributed to the higher thermal conductivity of salts. Chemical reactions also occur in these two cases under the effects of thermal gradients, and the concentration of the precipitated salts are respectively 1500 and 4509 mmol l^{-1} (figures 5 and 6). According to equation (1), the porosity of rocks declines with growing salt precipitation. The porosity of areas near the salt diapir of the first and second cases is respectively 0.08 and 0.095, while that far away from the salt diapir is about 0.1 (figures 7–9).

The porosity is defined as a function of mineral concentration, and decreases with the growth of salt precipipation. Since the salt precipitation concentrates in the areas close to the salt diapir, the porosity of these areas declines by higher magnitudes. Figure 9 shows that the gradient orientation of porosity is horizontal for the three time scales. At the end of the simulation, namely after 10 My from the beginning, the porosity along the salt diapir decreases from 0.1 to 0.067, and in the meantime, the porosity 10 km from the salt diapir drops from 0.1 to 0.9. As for the cases with a time scale of 3.3 My and 6.6 My, the porosity of areas adjacent to the salt diapir respectively falls from 0.1 to 0.097 and 0.088.

Figure 10 shows porosity variations with reference to the vertical direction of the three cases. After 10 My, the porosity near the salt diapir rolls down from the initial value of 0.1 to 0.07. For the cases with time scales of 3.3 My and 6.6 My, the near-salt-diapir porosity declines respectively from 0.1 to 0.092 and 0.097.

Discussion and conclusions

Results show that overpressured salt-anhydrite formations have higher pressure heads. The two species elements sodium and chlorite are transported into the porous sedimentary rocks through water influx (saturated brine). The influx fluids flow horizontally through the interface between the salt dome and sedimentary formations, which correspondingly creates migration paths. The temperatures of areas close to the salt diapir are much lower than those away from the salt diapir, due to the higher thermal conductivity of salts. Halite precipitation occurs as sodium and chlorite are delivered into a cooler environment by the brine.

The concentration of the relevant species (sodium, chlorite and precipitated salts) are varied in different positions, since salt precipitation is dominated by temperatures, and temperatures differentiate from each other in different places. Because the temperatures near the salt diapir are lower than those of other parts of the model, the brine flowing into such areas cools and salt precipitation occurs subsequently. Numerical simulations have been conducted to evaluate salt precipitation induced by thermal gradients. Salt precipitation was simulated using the SHEMAT-Suite. The temperatures close to the salt diapir are different from those of the sedimentary reservoir formations, and thermally induced mineral precipitation occurs in places close to the salt diapir, which changes the porosity of the formations. After 10 My, the porosity along the salt diapir in the sedimentary Layer H1 decreases by 30%. Moreover, salt precipitation fades with increasing distance to the salt diapir, and so does porosity. Variations in mineral concentration/cementation in the pore space with different distances to the salt diapir are expected. Porosity declines more as time elapses. Salt cementation of reservoir rocks leads to falling porosity and permeability near salt domes, and formation cementation decreases with extending distances to the salt diapir. In addition, precipitation and resultant porosity decline related to the scaling problems in geothermal engineering can also be evaluated in the approach practiced in this paper.

Acknowledgments

We thank the guidance and contribution of Prof C Clauser, Dr G Marquart, Dr A Ebigbo and Dr J Niederau in the Applied Geophysics and Geothermal Energy institute of RWTH Aachen University and Dr L Reuning in the Geological institute of RWTH Aachen University during one of the authors' post-doc period. S Li is funded by the startup project of China University of Petroleum, Beijing (No. 2462014YJRC041) and supported by Science Foundation of China University of Petroleum, Beijing (No. C201601). Y Wang is supported by the National Natural Science Foundation of China under Grant No. 11465017.

References

Bartels J, Kühn M, Schneider W, Clauser C, Pape H, Meyn V and Lajczak I 2002 Core flooding laboratory experiment validates numerical simulation of induced permeability change in reservoir sandstone *Geophys. Res. Lett.* **29** 34.1–4

Battistelli A, Calore C and Pruess K 1997 The Simulator TOUGH2/EWASG for modelling geothermal reservoirs with brines and non-condensible gas *Geothermics* **26** 437–64

Clauser C (ed) 2003 *Numerical Simulation of Reactive Flow in Hot Aquifers—SHEMAT and Processing SHEMAT* (Heidelberg: Springer)

Clauser C, Giese P, Huenges E, Kohl T, Lehmann H, Rybach L, Šafanda J, Wilhelm H, Windloff K and Zoth G 1997 The thermal regime of the crystalline continental crust: implications from the KTB *J. Geophys. Res.* **102** 18417–41

Clauser C and Villinger H 1990 Analysis of conductive and convective heat transfer in a sedimentary basin, demonstrated for the Rheingraben *Geophys. J. Int.* **100** 393–414

Dronkert H and Remmelts G 1996 Influence of salt structures on reservoir rocks in Block L2, Dutch continental shelf *Geology of Gas and Oil Under The Netherlands* ed H E Rondeel *et al* (Boston, MA: Kluwer) pp 159–66

Kukla P A, Reuning L, Becker S, Urai J L, Schoenherr J and Rawahi Z 2011 Distribution and mechanisms of overpressure generation and deflation in the Neoproterozoic to early Cambrian South Oman Salt Basin *Geofluids* **11** 349–61

Kühn M, Bartels J and Iffland J 2002 Long term behaviour of reservoir properties of a geothermally used aquifer—interaction between flow, heat transfer, transport, and chemical reactions *Geothermics* **31** 725–49

Kühn M, Frosch G, Kölling M, Kellner T, Althaus E and Schulz H D 1997 Experimentelle untersuchungen zur barytübersättigung einer thermalsole *Grundwasser* **3** 111–7 (with English abstract)

Kühn M and Pape H 2003 *4th Chapter-Chemical Model in SHEMAT and Processing SHEMAT* (Heidelberg: Springer)

Kühn M, Vernoux J-F, Isenbeck-Schröter M, Kellner T and Schulz H D 1998 On-site experimental simulation of brine injection into a clastic reservoir as applied to geothermal exploitation in Germany *Appl. Geochem.* **13** 477–90

Pape H, Clauser C and Iffland J 1999 Permeability prediction for reservoir sandstones based on fractal pore space geometry *Geophysics* **64** 1447–60

Pape H, Clauser C and Iffland J 2000 Permeability–porosity relationship in sandstone based on fractal pore space geometry *Pure Appl. Geophys.* **157** 603–19

Prakash M 2013 Numerical studies on natural convection heat losses from open cubical cavities *J. Eng.* **2013** 320647

Purvis K and Okkerman J A 1996 Inversion of reservoir quality by early diagenesis: an example from the Triassic Buntsandstein, offshore Netherlands *Geology of Gas and Oil Under The Netherlands* ed H E Rondeel *et al* (Dordrecht: Kluwer) pp 179–89

Reuning L, Schoenherr J, Heimann A, Urai J L, Littke R, Kukla P and Rawahi Z 2009 Constraints on the diagenesis, stratigraphy and internal dynamics of the surface-piercing salt domes in the Ghaba Salt Basin (Oman): a comparison to the Ara formation in the South Oman Salt Basin *GeoArabia* **14** 83–120

Strozyk F, van Gent H, Urai J L and Kukla P A 2012 3D seismic study of complex intra-salt deformation: an example from the

Upper Permian Zechstein 3 stringer, western Dutch offshore *Salt Tectonics, Sediments and Prospectivity* (*Geological Society of London Special Publications* vol 363) ed G I Alsop *et al* (London: The Geological Society) pp 489–501
Swain I, Mishra S R and Pattanayak H B 2015 Flow over exponentially stretching sheet through porous medium with heat source/sink *J. Eng.* **2015** 452592
Van Bergen F and Deleeuw C S 2001 Salt cementation of reservoir rocks near salt domes in the Netherlands North Sea area—a new mechanism *EAGE 63rd Conf. & Technical Exhibition (Amsterdam, The Netherlands, 11–15 June 2001)*
Van Gent H, Urai J L and De Keijzer M 2011 The internal geometry of salt structures—a first look using 3D seismic data from the Zechstein of the Netherlands *J. Struct. Geol.* **33** 292–311